Fourier summation, FORDAP; least-squares refinement, ORXLFS3; error analysis of distances and angles, ORFEE3; structural drawings, ORTEPII. For the intensity statistics MULTAN was used; J. P. Declercq, G. Germain, P. Main, and M. M. Woolfson, *Acta Crystallogr., Sect. A*, **29**, 231 (1973).
(17) C. Peters and C. F. Eagen, *Phys. Rev. Lett.*, **34**, 1132 (1975); *Inorg. Chem.*, **15**, 782 (1976); H. J. Deiseroth and H. Schulz, *Phys. Rev. Lett.*, **33**, 963 (1974); *Mater. Res. Bull.*, **10**, 225 (1975); G. Heger, B. Renker, H. J. Deiseroth, H. Schulz, and G. Scheiber, *ibid.*, **10**, 217 (1975).
(18) G. E. Bacon, *Acta Crystallogr., Sect. A*, **8**, 357 (1972).
(19) R. B. Saillant, R. C. Jaklevic, and C. D. Bedford, *Mater. Res. Bull.*, **9**, 289 (1974).
(20) A. J. Schultz, G. D. Stucky, J. M. Williams, T. R. Koch, and R. L. Maffly, *Solid State Commun.*, **21**, 197 (1977).
(21) P. L. Johnson, A. J. Schultz, A. E. Underhill, D. M. Watkins, D. J. Wood, and J. M. Williams, *Inorg. Chem.*, following paper in this issue; J. M. Williams, P. L. Johnson, and A. E. Underhill, Abstracts, American Crystallographic Association Meeting, Asilomar, Calif., 1977 No. HA 6.
(22) L. Pauling, "The Nature of the Chemical Bond and the Structure of Molecules and Crystals", Cornell University Press, Ithaca, N.Y., 1960, pp 398–404.
(23) R. Comès, M. Lambert, H. Launois, and H. R. Zeller, *Phys. Rev. B*, **8**, 571 (1973).
(24) For a review see G. D. Stucky, A. J. Schultz, and J. M. Williams, *Annu. Rev. Mater. Sci.*, **7**, 301 (1977).
(25) Private communication with H. R. Zeller, Brown Boveri Research Center, Baden, Switzerland.
(26) The 1.4-mg crystal data set also yielded unequal Pt–Pt spacings (2.887 (17) and 2.915 (17) Å) but the esd's were approximately twice those derived from the 14.9-mg crystal data set. Only distances and angles for crystal II are given.
(27) (a) Private communication with J. R. Miller, Xerox Research, Webster, N.Y. (b) See footnote 15 of T. Takahashi, H. Akagawa, H. Doi, and H. Nagasawa, *Solid State Commun.*, **23**, 809 (1977). (c) S. Drosdziok and M. Engbrodt, *Phys. Status Solidi B*, **72**, 739 (1975). (d) See ref 25.

Contribution from the Chemistry Division, Argonne National Laboratory, Argonne, Illinois 60439, and School of Physical and Molecular Sciences, University College of North Wales, Bangor, Wales

Structural Studies of Precursor and Partially Oxidized Conducting Complexes. 15. A Combined Neutron and X-Ray Diffraction Study of Ammonium Tetracyanoplatinate Chloride Trihydrate, $(NH_4)_2[Pt(CN)_4]Cl_{0.3}\cdot 3H_2O$[1]

PAUL L. JOHNSON,[2a] ARTHUR J. SCHULTZ,[2a] ALLAN E. UNDERHILL,[2b] DAVID M. WATKINS,[2b] DAVID J. WOOD,[2b] and JACK M. WILLIAMS*[2a]

Received September 27, 1977

The crystal and molecular structure of one-dimensional ammonium tetracyanoplatinate chloride trihydrate, $(NH_4)_2[Pt(CN)_4]Cl_{0.3}\cdot 3H_2O$, $NH_4CP(Cl)$, has been elucidated in detail using single-crystal neutron and x-ray diffraction techniques. The compound $NH_4CP(Cl)$ crystallizes with two molecules in the tetragonal cell C_{4v}^1-*P4mm* of (neutron, x ray) dimensions a = 10.048 (7), 10.087 (5) Å and c = 5.861 (4), 5.840 (2) Å, respectively. The x-ray diffraction study was undertaken in order to alleviate the problem of large NH_4^+ ion thermal motion and resultingly large esd's obtained for the Pt–Pt intrachain distances derived in the neutron diffraction study. It is likely that only a low-temperature neutron diffraction investigation will reduce the NH_4^+ ion motion sufficiently to allow us to derive more precise Pt–Pt distances. In the neutron diffraction experiment, a total of 811 reflections were averaged to yield 390 independent reflections (312 with $F_o^2 > 1\sigma(F_o^2)$). The x-ray diffraction data set consisted of 340 independent reflections of which 307 had $F_o^2 > 1\sigma(F_o^2)$. The structure is isomorphous with that of the prototype one-dimensional conductor $K_2[Pt(CN)_4]Br_{0.3}\cdot 3H_2O$, KCP(Br). Using full-matrix least-squares techniques, the final refinement yielded $R(F_o^2)$ values (neutron, x ray) of 0.131 and 0.122. The structure consists of linear Pt–Pt chains arising from the stacking of square-planar $Pt(CN)_4^{1.7-}$ groups. Adjacent $Pt(CN)_4^{1.7-}$ moieties have a staggered configuration yielding a C–Pt–Pt–C torsion angle of 45°. The Pt–Pt spacings are *different* at 2.914 (26) and 2.947 (26) Å (neutron) and (more precise) 2.910 (5) and 2.930 (5) Å (x rays). The average Pt–Pt separation (2.92 Å) in $NH_4CP(Cl)$ is ~0.04 Å longer than that observed in KCP(Br). The combined effects of the increased, and now *unequal*, intrachain Pt–Pt separations in $NH_4CP(Cl)$ appear to be the main cause of its diminished conductivity compared to KCP(Br). From the neutron diffraction data, we find that three of the four NH_4^+ group hydrogen atoms participate in hydrogen bonding interactions thereby resulting in formation of NH···$^-$N≡C and one NH···O bonds. The neutron and x-ray diffraction data yield different results regarding placement of the Cl^- ion. The neutron data may be interpreted in terms of a "two-site" model for the Cl^- ion, at (0.5, 0.5, 0.4838) and (0.5, 0.5, 0.6055), which yields a derived total Cl^- occupancy factor of 0.41 (18). This value is not significantly different from the accepted value of 0.30 for KCP(Br), KCP(Cl), and RbCP(Cl) and therefore a value of 0.30 has been adopted for this study (vide infra). The x-ray data provide evidence for only one Cl^- ion at (0.5, 0.5, 0.5). However, the Cl^- occupancy factor could not be refined, using least-squares techniques, to a reasonable value.

Introduction

One-dimensional partially oxidized tetracyanoplatinate (POTCP) conductors continue to be of interest not only because they have anisotropic electrical properties but also because metal bond formation produces short metal–metal spacings (typically ~0.1–0.2 Å longer than in Pt metal).[3] However, the crystalline environment about the metal-atom chains influences the one-dimensional conduction properties and associated phenomena, such as Peierls' distortions and charge density wave formation. By varying the ligands, cations, anions, and degree of lattice hydration, one should observe a discernible, logical, and predictable pattern of varying electrical conductivity.

Variable-temperature conductivity studies of four such closely related POTCP compounds have been reported by Underhill et al.,[4] viz., $M_2[Pt(CN)_4]Cl_{0.3}\cdot 3H_2O$, $M^+ = K^+$, Rb^+, and NH_4^+, and "$(NH_4)_{2.2}[Pt(CN)_4]Cl_{0.5}\cdot 3H_2O$". Although it was assumed that these one-dimensional salts all possess similar crystal structures and because Rb^+ and NH_4^+ have nearly identical ionic radii (~1.48 Å), the conductivity studies indicated a surprising trend, viz., K > Rb > NH_4 in MCP(Cl). $NH_4CP(Cl)$ is of additional interest because of the distinct possibility that it contains *unequal* intrachain Pt–Pt separations as we have recently observed in $Rb_2[Pt(CN)_4]Cl_{0.3}\cdot 3H_2O$.[6] As reported elsewhere the NH_4^+ ion containing materials pose troublesome synthetic problems.[4,5,15] Finally the possibility of hydrogen bond formation between NH_4^+ ions and lattice water molecules is of interest because such interactions might serve to increase interchain coupling thereby rendering thermal breakdown of the correlated Peierls distortion more difficult.

In this paper we report the results of a combined neutron and x-ray diffraction single-crystal structural investigation of $(NH_4)_2[Pt(CN)_4]Cl_{0.3}\cdot 3H_2O$. The structural results provide

0020-1669/78/1317-0839$01.00/0

evidence which suggest that diminished conductivity in this class of POTCP materials parallels an increase in Pt–Pt separations. Finally, the neutron diffraction results allow us to discuss the nature of the NH_4^+ hydrogen bonding interactions in $NH_4CP(Cl)$.

Experimental Section

Crystal Preparation. Initially, K_2PtCl_4 (Johnson Matthey & Co., Ltd.) was twice recrystallized from water and was then converted into $K_2Pt(CN)_4 \cdot 3H_2O$ with KCN. The $K_2Pt(CN)_4$ was converted into $H_2Pt(CN)_4$ under N_2 using a Dowex 50W-X8 cation-exchange resin. The acid was rotary evaporated to an oil, with only gentle warming to avoid decomposition. The acid was then neutralized with dilute ammonia solution (analytical grade) and one-sixth of the solution was saturated with chlorine. Both this solution and the remaining five-sixths of the original solution were then separately evaporated to dryness with gentle heating (<30 °C) to remove excess chlorine and ammonia, respectively. The resulting solids were dissolved in a little water to give almost saturated solutions. NH_4Cl and water were added until the resulting solution was approximately 3.7 M in NH_4Cl and 0.5 M in the platinum salt. The solution was filtered through a Millex 0.45 μM filter and was allowed to evaporate slowly at 20 °C to yield large crystals.

Unit Cell and Space Group. Preliminary x-ray diffraction measurements indicated that $NH_4CP(Cl)$ is isostructural with tetragonal KCP(Br, Cl).[7] Unit cell constants were established for the neutron diffraction study by centering 18 reflections in the range $35 < 2\theta < 60°$. A least-squares fit of the angles 2θ, χ, and ϕ (neutron wavelength 1.142 (1) Å at 22 °C) yielded $a = 10.048$ (7) and $c = 5.861$ (4) Å. These may be compared with those for $K_2[Pt(CN)_4]Br_{0.3} \cdot 3H_2O$[7] and $K_2[Pt(CN)_4]Cl_{0.3} \cdot 3H_2O$[8] which are $a = 9.907$ (3), 9.883 (3) Å and $c = 5.780$ (2), 5.748 (2) Å, respectively. All least-squares refinements were conducted using space group $P4mm$ (C_{4v}^1). The calculated crystal density for two formula units per unit cell is 2.304 g cm^{-3} and the observed value, determined by flotation in methyl iodide and bromoform, is 2.28 (1) g cm^{-3}.

Neutron Data Collection. A fully automated Electronics and Alloys four-circle diffractometer located at the CP-5 research reactor of Argonne National Laboratory was used to collect neutron diffraction data (λ 1.142 (1) Å). The diffractometer is operated under the remote control of the Chemistry Division Sigma V computer.[9] The monochromatic beam results from the use of a Be single-crystal monochromator, with monochromator angle $\theta_m = 30°$, yielding a neutron flux of $\sim 2.9 \times 10^6$ N cm^{-2} s^{-1}.

A θ–2θ step-scan technique was used to collect data (step size equals 0.1° in 2θ). Backgrounds were established at each extremity of the scan with the crystal and counter in a stationary position. A total of 811 reflections were collected to a minimum d spacing of 0.808 Å. These reflections were averaged over equivalent forms to yield 390 unique data of which 312 had $F_o^2 > 1\sigma(F_o^2)$. Instrument and crystal stabilities were monitored by remeasuring two standard reflections every 80 measurements; their combined intensities did not vary more than 5% during data collection.

Structure factors were derived by applying Lorentz and absorption corrections ($\mu_{calcd} = 2.33$ cm^{-1}) and the resulting transmission factors ranged from 0.63 to 0.75. By use of the absorption-corrected integrated intensities the F_o^2 were obtained by application of the following equation:[10] $F_o^2 = (\omega I \sin 2\theta)/I_0\lambda^3 N^2 V$, where I_0 is the incident intensity, λ is the wavelength, ω is the angular velocity of rotation of the crystal, N is the number of unit cells per unit volume, V is the specimen volume, and θ is the Bragg angle. A cylindrical NaCl crystal, for which precise absorption and secondary extinction corrections had been made, was used to obtain I_0 and thereby place the F_o^2 on an approximately "absolute scale". The variances of F_o^2 were calculated from $\sigma^2(F_o^2) = \sigma_c^2(F_o^2) + (0.05F_o^2)^2$, where $\sigma_c^2(F_o^2)$ is determined from the counting statistics and 0.05 is an added factor to account for the 5% maximum variation in the integrated intensities of the standard reflections.

X-Ray Data Collection. A crystal of $NH_4CP(Cl)$ measuring 0.16 × 0.16 × 0.34 mm was mounted on a Syntex $P2_1$ four-circle computer-controlled diffractometer with graphite-monochromatized Mo Kα radiation (λ 0.7107 Å). The refined cell constants were $a = 10.087$ (5) Å and $c = 5.840$ (2) Å.

Intensity data were collected using the θ–2θ scan technique. The scan range was from $[2\theta(\text{Mo K}\alpha_1) - 1.0°]$ to $[2\theta(\text{Mo K}\alpha_2) + 1.0°]$. Backgrounds ($B_1$ and B_2) were measured both at the beginning and at the end of the scan, each for half of the total scan time. Three reference reflections were monitored every 80 measurements to observe crystal movement or decomposition; the maximum deviation of the standards from the average was 3%.

Table I. Final Discrepancy Factors (Neutron Data) for $(NH_4)_2[Pt(CN)_4]Cl_{0.3} \cdot 3H_2O$[a]

Data selection	No. of reflections	$R(F_o)$	$R(F_o^2)$	$R_w(F_o^2)$	σ_1
All data	390	0.115	0.131	0.120	1.31
Reflections with $F_o^2 > 1.0\sigma(F_o^2)$	312	0.085	0.121	0.115	1.46

[a] See Neutron Structure Solution and Refinement section for explanation of $R(F_o)$, $R(F_o^2)$, $R_w(F_o^2)$, and σ_1.

The net intensity and its standard deviation ($\sigma(I)$) were calculated from

$$I = SC - (B_1 + B_2)$$

$$\sigma(I) = [SC + (B_1 + B_2) + P^2I^2]^{1/2}$$

where SC is the count during the scan and P (a factor to account for systematic error) was set equal to 0.03.

Structure factors were derived by applying Lorentz, polarization, and absorption corrections. The calculated transmission factors ($\mu_{calcd} = 130.3$ cm^{-1}) ranged from 0.13 to 0.18.

Neutron Structure Solution and Refinement.[11] A starting point for the solution of this structure was the assumption of isomorphism with KCP(Br) with the NH_4^+ substituting for K^+. Initial full-matrix least-squares refinement of the nonhydrogen atom positional parameters, with isotropic thermal parameters, yielded discrepancy indices as follows:

$$R(F_o) = \frac{\Sigma||F_o| - |F_c||}{\Sigma|F_o|} = 0.27$$

$$R(F_o^2) = \frac{\Sigma|F_o^2 - F_c^2|}{\Sigma F_o^2} = 0.34$$

and

$$R_w(F_o^2) = \left[\frac{\Sigma w_i|F_o^2 - F_c^2|^2}{\Sigma w_i F_o^4}\right]^{1/2} = 0.39$$

Inspection of a difference Fourier map yielded the locations of all NH_4^+ ion hydrogen atoms. The presence of a "second site" for the Cl^- ion was also revealed by the difference maps.

Full-matrix least-squares refinement was continued by varying all positional parameters, anisotropic temperature factors, a scale factor, and the occupancy factors for the Cl^- ions in the main and secondary site. This refinement did not proceed smoothly in that the hydrogen atoms tended to yield nonpositive definite temperature factors. A converged refinement was eventually achieved by damping the parameter shifts on the hydrogen atoms, the chlorine atoms, and C(2). The large apparent thermal motion of the NH_4^+ H atoms appeared to be the origin of this problem.

The final refinements gave the agreement figures listed in Table I. The final positional and thermal parameters for the neutron diffraction study are given in Table II. The standard deviation of an observation of unit weight

$$\sigma_1 = \left[\frac{w_i|F_o^2 - F_c^2|^2}{n - p}\right]^{1/2}$$

where n is the number of observations and p is the number of parameters (93) in the least-squares refinement, was 1.31. The final observation to parameter ratio was 4.2:1.

In order to provide a check of the final least-squares refinement, a difference Fourier map was calculated. The largest peak had intensity only 4% that of a Pt peak and was located at ($^1/_2$, $^1/_2$, −0.052). Although the scattering density was negative, it was not in a logical position for a hydrogen atom. The next 15 largest peaks were of intensity only 20% above the background level. The final derived Cl^-

Table II. Positional and Thermal Parameters for $(NH_4)_2[Pt(CN)_4]Cl_{0.3}\cdot 3H_2O$ and Root-Mean-Square Displacements (in A) of Atoms along Their Principal Ellipsoidal Axes from the Neutron Diffraction Study[a,b]

Atom	10^4x	10^4y	10^4z	$10^4\beta_{11}$	$10^4\beta_{22}$	$10^4\beta_{33}$	$10^4\beta_{12}$	$10^4\beta_{13}$	$10^4\beta_{23}$	$10^3\mu_1$	$10^3\mu_2$	$10^3\mu_3$
Pt(1)	0	0	0	56 (9)	56	146 (24)	0	0	0	159 (14)	169 (15)	169 (15)
Pt(2)	0	0	5029 (40)	55 (10)	55	134 (23)	0	0	0	153 (14)	167 (16)	167 (16)
C(1)	1987 (6)	0	−5 (48)	54 (6)	89 (6)	218 (18)	0	−42 (23)	0	139 (24)	214 (8)	215 (18)
C(2)	1400 (7)	1400	5045 (42)	61 (7)	61	185 (18)	−18 (5)	0	0	148 (10)	180 (9)	201 (8)
N(1)	3127 (5)	0	−3 (44)	62 (5)	145 (7)	334 (20)	0	−47 (20)	0	161 (14)	253 (12)	272 (7)
N(2)	2208 (7)	2208	5057 (41)	100 (7)	100	299 (16)	−30 (4)	−37 (30)	−37	163 (20)	248 (13)	258 (7)
N(3)	1959 (11)	5000	7481 (48)	141 (11)	93 (9)	604 (56)	0	50 (23)	0	218 (11)	257 (13)	333 (17)
Cl(1)	5000	5000	4838 (337)	39 (84)	39	161 (500)	0	0	0	141 (160)	141 (166)	167 (280)
Cl(2)	5000	5000	6055 (311)	132 (86)	132	360 (424)	0	0	0	250 (159)	260 (92)	260 (92)
O(1)	5000	0	3743 (47)	84 (21)	336 (48)	328 (73)	0	0	0	207 (28)	239 (29)	415 (32)
O(2)	3448 (31)	3448	1028 (48)	205 (28)	205	312 (45)	−23 (22)	90 (46)	90	176 (41)	341 (18)	341 (17)
H(1)	4239 (25)	0	2692 (54)	159 (29)	301 (40)	355 (82)	0	−107 (51)	0	196 (39)	324 (33)	392 (29)
H(2)	3013 (60)	3013	1986 (81)	253 (78)	253	731 (147)	47 (42)	176 (132)	176	255 (42)	325 (36)	464 (55)
H(3)	3899 (67)	3899	1630 (103)	541 (194)	541	937 (353)	−353 (112)	106 (148)	106	271 (49)	430 (78)	676 (82)
H(4)	1683 (31)	4361 (31)	8208 (56)	398 (60)	306 (54)	612 (111)	−113 (38)	−28 (60)	85 (53)	304 (35)	358 (32)	496 (37)
H(5)	2739 (46)	5000	7612 (160)	237 (57)	311 (73)	3437 (737)	0	−611 (185)	0	244 (49)	399 (51)	812 (94)
H(6)	1550 (67)	5000	5954 (62)	638 (161)	728 (169)	152 (66)	0	113 (89)	0	151 (41)	574 (78)	610 (77)

[a] The estimated standard deviations in parentheses for this and all subsequent tables refer to the least significant figures. [b] The form of the temperature factor is $\exp[-(\beta_{11}h^2 + \beta_{22}k^2 + \beta_{33}l^2 + 2\beta_{12}hk + 2\beta_{13}hl + 2\beta_{23}kl)]$.

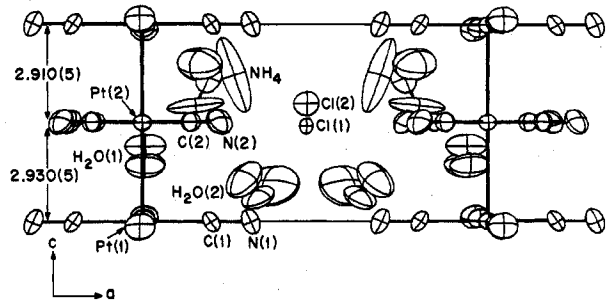

Figure 1. Drawing of a half-unit cell (50% probability ellipsoids) of $(NH_4)_2[Pt(CN)_4]Cl_{0.3}\cdot 3H_2O$ showing the linear Pt atom chains, the *unequal* Pt–Pt separations, and the asymmetric placement of H_2O molecules and NH_4^+ ions in different halves of the unit cell. The drawing of the thermal ellipsoids is based on the neutron diffraction data while the Pt–Pt spacing is from the x-ray diffraction experiment (see text and Table IVA).

sites and occupancy factors are discussed in Table V.

For the least-squares refinements, the coherent neutron scattering amplitudes which were used for Pt, C, N, O, Cl, and H were respectively 0.95, 0.663, 0.94, 0.575, 0.958, and −0.372, all in units of 10^{-12} cm.[12]

X-Ray Diffraction Structure Solution and Refinement. The Pt, C, N, and O atom positional parameters derived from the neutron diffraction study were used to calculate a difference Fourier map which indicated the presence of only one (Cl^-) peak at (0.5, 0.5, 0.5). Final positional and thermal parameters for the x-ray study are given in Table III. In contrast to the neutron diffraction result, there was *no* second site for the Cl^- atom. After introduction of this atom the $R(F_o^2) = 0.075$. However, the atom multiplier consistently refined to an impossibly large value of 0.73 (2) whereas the maximum chemical occupancy allowed at (0.5, 0.5, z) is 0.5. A final difference Fourier map calculated at this point was virtually featureless with the largest peak corresponding to 1.3 e/Å^3. These results strongly suggest the presence of a higher atomic number scatterer at this site. Therefore, although Br^- contamination was very unlikely, a least-squares refinement in which the Cl^- scattering factor table was replaced by Br^- led to the following results: (i) $R(F_o^2)$ increased radically from 0.075 to 0.243, (ii) B_{Br} dropped to an unreasonable value of 0.36 (79), and (iii) the Pt-atom temperature factors became nonpositive definite. Similar calculations using a scattering factor table corresponding to (0.5Cl + 0.5Br) led to a diverged refinement [$R(F_o^2) = 0.77$], and several atom temperature factors became nonpositive definite. The final x-ray refinement was achieved by restricting the Cl^- site to a chemical occupancy of 0.35 and an isotropic B value of 3.0 Å^2 resulting in a final $R(F_o^2)$ of 0.122. In these calculations the atomic scattering factors were as listed in ref 13. A final difference Fourier map yielded a single peak of height 17.7 e/Å^3, located at (0.5, 0.5, 0.4976), which may indicate that either a more complicated (and nonresolvable) Cl^- disorder exists than is contained in the present structural model or this site is occupied by a larger atomic number anion. There was therefore no clear indication that a scattering center with lower atomic number than Cl^-, such as a "defect" water molecule,[14] could be associated with either Cl^- site. The "defect" water molecule hypothesis seems even more unlikely in terms of the recent results[6] which demonstrate that KCP(Br) and RbCP(Cl) are definitely 3.0 hydrates as opposed to the one reported value for KCP(Br) of 3.2.[14] An additional possibility is electron charge buildup due to charge density wave formation. However, such a hypothesis is difficult to verify.

Structure Description

The Linearly Dimerized Pt-Atom Chain. As in previously studied POTCP salts in which the Pt-atom valence is +2.3 to +2.4, the square-planar $Pt(CN)_4^{1.x-}$ groups stack to form linear Pt-atom chains parallel to c (see Figure 1). In $NH_4CP(Cl)$ the intrachain metal atom separations, which are independent in noncentrosymmetric space group $P4mm$, are *unequal* at 2.910 (5) and 2.930 (5) Å (x ray, see Table IVA). In isostructural RbCP(Cl)[6] the Pt atom separations are also longer than in KCP(Br) (2.88 (1) Å), and of unequal length (2.924 (8) and 2.877 (8) Å). Therefore, insertion of nearly equally sized Rb^+ or NH_4^+ ions, the latter being that which can form

Table III. Positional and Thermal Parameters ($\times 10^4$) from the X-Ray Diffraction Study of $(NH_4)_2[Pt(CN)_4]Cl_{0.3}\cdot 3H_2O$[a]

Atom	x	y	z	β_{11}	β_{22}	β_{33}	β_{12}	β_{13}	β_{23}
Pt(1)	0	0		35 (5)	35	86 (12)	0	0	0
Pt(2)	0	0	5018 (9)	41 (6)	41	97 (12)	0	0	0

Atom	x	y	z	B,[b] Å^2	Atom	x	y	z	B,[b] Å^2
C(1)	2043 (32)	0	14 (86)	1.3 (5)	N(3)	1929 (10)	5000	7505 (45)	3.0 (2)
C(2)	1447 (43)	1447	4906 (72)	1.0 (5)	O(1)	5000	0	4378 (78)	2.4 (9)
N(1)	3197 (32)	0	−23 (73)	2.5 (6)	O(2)	3474 (71)	3474	825 (85)	6.0 (12)
N(2)	2264 (48)	2264	5015 (104)	2.5 (5)	Cl	5000	5000	5299 (80)	3.0[c]

[a] The form of the temperature factor is $\exp[-(\beta_{11}h^2 + \beta_{22}k^2 + \beta_{33}l^2 + 2\beta_{12}hk + 2\beta_{13}hl + 2\beta_{23}kl)]$. [b] Isotropic temperature factor is of the form $\exp(-B(\sin^2\theta)/\lambda^2)$. [c] This parameter could not be refined; it was fixed at 3.0.

Table IV. Interatomic Distances (Å) and Bond Angles (deg) for $(NH_4)_2[Pt(CN)_4]Cl_{0.3}\cdot 3H_2O$

(A) Distances around Platinum Atoms

Pt(1)-C(1)	1.997 (6)	Pt(1)-Pt(2)	2.930 (5)[b]
Pt(2)-C(2)	1.990 (6)	Pt(1)-Pt(2)^{I}	2.910 (5)[b]

(B) Carbon-Nitrogen Distances in Cyanide Groups

C(1)-N(1)	1.145 (7)	C(2)-N(2)	1.147 (6)

(C) Water Molecule Distances

O(1)-H(1)	0.982 (34)	O(2)-H(3)	0.733 (68)
O(2)-H(2)	0.835 (59)		

(D) Hydrogen Atom Interactions[a]

H(1)-N(1)	1.935 (25)	O(1)-H(1)-N(1)	164.1 (27)
H(2)-N(2)	2.133 (41)	O(2)-H(2)-N(2)	164.8 (47)
H(3)-Cl(1)	2.446 (183)	O(2)-H(3)-Cl(1)	158.6 (59)
H(4)-N(1)^{II}	2.345 (31)	N(3)-H(4)-N(1)	153.1 (32)
H(6)-O(1)^{III}	2.026 (67)	N(3)-H(6)-O(1)	154.5 (52)

(E) Ammonium Ion Distances

N(3)-H(4)	0.819 (38)	N(3)-H(6)	0.985 (49)
N(3)-H(5)	0.787 (54)		

(F) Ammonium Ion Interactions

N(3)-O(1)^{III}	2.946 (25)	N(3)-N(1)^{VI}	3.097 (13)
N(3)-O(2)^{IV}	2.998 (24)	N(3)-N(2)	3.155 (10)
N(3)-O(2)^{V}	2.998 (24)	N(3)-N(2)^{VII}	3.155 (10)
N(3)-N(1)^{II}	3.097 (13)	N(3)-Cl(1)	3.426 (97)

(G) Chloride Ion Interactions

Cl(1)-O(2)	3.139 (150)	Cl(1)-N(3)^{III}	3.426 (97)
Cl(1)-O(2)^{VIII}	3.139 (150)	Cl(1)-N(3)^{X}	3.426 (97)
Cl(1)-O(2)^{IX}	3.139 (150)	Cl(2)-N(3)	3.168 (53)
Cl(1)-O(2)^{VII}	3.139 (150)	Cl(2)-N(3)^{VIII}	3.168 (53)
Cl(1)-N(3)	3.426 (97)	Cl(2)-N(3)^{III}	3.168 (53)
Cl(1)-N(3)^{VIII}	3.426 (97)	Cl(2)-N(3)^{X}	3.168 (53)

(H) Angles of Pt Chain and Bonded Atoms

Pt(2)-Pt(1)-Pt(2)^{I}	180	H(4)^{VII}-N(3)-H(5)	106.6 (45)
Pt(1)-C(1)-N(1)	179.9 (16)	H(5)-N(3)-H(5)	106.6 (45)
Pt(2)-C(2)-N(2)	180.0 (18)	H(4)-N(3)-H(6)	120.3 (76)
C(1)-Pt(1)-C(1)^{III}	90.000 (2)	H(4)-N(3)-H(4)^{VII}	103.3 (45)
C(2)-Pt(2)-C(2)^{XI}	90.00 (32)	H(4)-N(3)-H(6)	109.3 (26)
H(1)-O(1)-H(1)^{VIII}	102.3 (40)	H(4)^{VII}-N(3)-H(6)	109.3 (26)
H(2)-O(2)-H(3)	108.9 (51)		

[a] All values were derived from the neutron diffraction study unless otherwise stated. [b] X ray. [c] Superscripts refer to symmetry positions listed below. If no superscript appears (x, y, z) is implied: (I) $x, y, z-1$; (II) $y, x, 1+z$; (III) y, x, z; (IV) $x, y, 1+z$; (V) $x, -y, 1+z$; (VI) $-y, 1-x, 1+z$; (VII) $x, 1-y, z$; (VIII) $1-x, 1-y, z$; (IX) $1-x, y, z$; (X) $1-y, 1-x, z$; (XI) $-x, y, z$.

Table V. Comparison of the Positional Parameters and Occupancy Factors of the Cl(1) and Cl(2) Sites in $NH_4CP(Cl)$[a] and KCP(Br)[b]

		$NH_4CP(Cl)$	KCP(Br)
Cl(1)	Position	(0.5, 0.5, 0.4838 (337))	(0.5, 0.5, 0.4976 (31))
	Crystallographic occupancy	0.038 (31)	0.063 (3)
Cl(2)	Position	(0.5, 0.5, 0.6055 (311))	(0.5, 0.5, 0.6574 (75))
	Crystallographic occupancy	0.064 (32)	0.023 (3)
Total Cl^- stoichiometry (calcd−chemical)		0.408 (178)	0.344 (12)

[a] Neutron diffraction data—this study. [b] Neutron diffraction data.[7]

H bonds, into the "KCP(Br)" structure results in an increase in Pt–Pt separation which is paralleled by diminished electrical conductivity along the metal atom chain. However, the alternately long and short sequence of Pt–Pt spacings is in reverse order to those observed in RbCP(Cl).

Since the main information regarding the x-ray study pertains to the derived Pt–Pt spacings discussed above, the remaining discussion of structure is based on the neutron diffraction results. Space group (*P4mm*) considerations require linear Pt-atom chain formation in $NH_4CP(Cl)$. Similar considerations require that the C–Pt–Pt–C torsion angles be fixed at 45° (see Figure 2). All bond distances and angles in the $Pt(CN)_4^{1.7-}$ moieties appear normal (see Table IV). Except for the Cl^- ion disorder (required by the chemical nonstoichiometry of $NH_4CP(Cl)$), the structure appears to be well ordered. Although the NH_4^+ ions show shortened N–H distances (Figure 4) due to large thermal motion, they do not appear to be disordered.

The Two Cl^- Sites. We have previously pointed out in the Neutron Refinement section that two anion sites, which we have ascribed to Cl^-, were observed. In Table V the derived positional parameters and site occupancy factors for Cl(1) and Cl(2) are compared with those derived previously for KCP(Br).[7] It should be pointed out that while KCP(Br) and $NH_4CP(Cl)$ both show very similar Cl(1) and Cl(2) positional parameters, the site occupancy factors are *reversed* (see Table V). However, because of the large esd's of the site occupancy factors, this reversal may be an artifact. The possibility that one of the Cl^- sites is due to a "defect water" molecule[14] cannot be ruled out using the present room-temperature neutron diffraction data. The environment about the Cl(1) site is similar to that in KCP(Br) in which four symmetry related O(2) atoms and four N(3) atoms complete the eightfold coordination (see Figure 3).

The environment about the chloride ion in the Cl(2) site can be described as the result of Cl(2) being shifted toward N(3). There are four symmetry related N(3) atoms 3.168 (53) Å away. The Cl(2)–Cl(1) distance is 0.713 (75) Å so the sites cannot be simultaneously occupied.

H_2O and NH_4^+ Hydrogen Bonding Interactions. The water molecule hydrogen atoms all participate in hydrogen bond formation; H(1) and H(2) form H bonds with N(1) and N(2), respectively. The N···H distances are 1.935 (25) and 2.133 (41) Å, respectively, while the O–H–N angles are 164.1 (27) and 164.8 (47)°. H(3) appears to be weakly bound to Cl(1). Three of the four hydrogen atoms on the ammonium ion participate in hydrogen bonding interactions while H(5) does not (see Table IVD). The H(4)···N(1) distance is 2.345 (31) Å and the N(3)—H(4)···N(1) bond angle is 153.1 (32)°. It should be noted that the N(3)–H(4) distance (0.819 (38) Å)

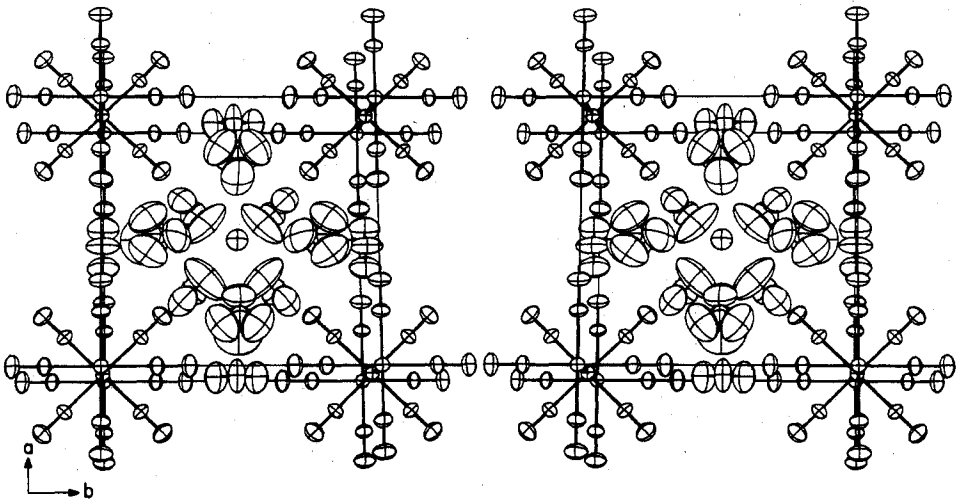

Figure 2. Stereodrawing of the structure of $(NH_4)_2[Pt(CN)_4]Cl_{0.3}\cdot 3H_2O$ viewed down the tetragonal *c* axis. Both Pt atom chains and the Cl^- ion form linear arrays parallel to *c*. All thermal ellipsoids are scaled to 50% probability.

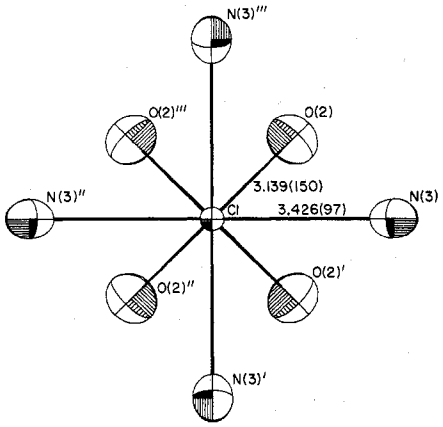

Figure 3. Diagram illustrating the chloride ion interactions at the Cl(1) site in $(NH_4)_2[Pt(CN)_4]Cl_{0.3}\cdot 3H_2O$.

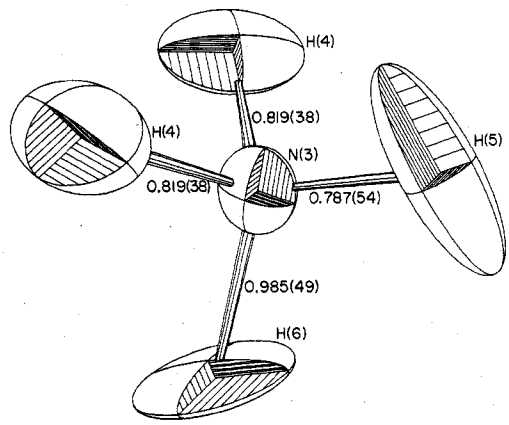

Figure 4. Drawing indicating the NH_4^+ ion N–H distances as determined by neutron diffraction. The N–H distances appear shortened due to thermal motion; only H(6) and H(4) participate in N—H···O and N–H···NC hydrogen bond formation (see text).

is abnormally short due to thermal motion which may cause the H(4)···N(1) distance to appear anomalously long. A stronger bond is formed by H(6)[N(3)—H(6)···O(1)] wherein the H(6)···O(1) distance is 2.026 (67) Å and the N(3)—H(6)···O(1) angle is 154.5 (52)°. A view of the NH_4^+ ion is presented in Figure 4.

The carbon atom configuration is square as shown by bond angles of C(1)–Pt(1)–C(1)′ of 90.000 (2)° and C(2)–Pt-(2)–C(2)′ of 90.00 (32)°. The canting of the CN^- ligands toward the NH_4^+ ion, which is pronounced in KCP(Br) and RbCP(Cl), is only slightly evident in this structure. The direction of the very slight CN^- canting that is observed parallels that in KCP(Br), i.e., directed away from the water molecules and toward the potassium or ammonium ion.

A least-squares plane through Pt(1) and the four symmetry related C(1) atoms found Pt(1) only 0.003 (30) Å out of the plane. Similarly Pt(2) was 0.009 (26) Å from the plane formed by the four symmetry related C(2) atoms.

Conclusions

The main structural findings reported here, which bear on the diminished electrical conductivity of $(NH_4)_2[Pt(CN)_4]$-$Cl_{0.3}\cdot 3H_2O$, compared to prototype $K_2[Pt(CN)_4]Br_{0.3}\cdot 3H_2O$, are that while the *intra*chain Pt–Pt spacings are shorter and are of equal length (2.88 (1) Å) in the K^+ salt, they are longer and are of different length (2.910 (5) and 2.930 (5) Å, x rays) in the NH_4^+ salt. Thus the formation of alternately long and short Pt–Pt separations (dimerization) in $NH_4CP(Cl)$ is likely one of the most important factors contributing to its electrical conduction properties. A factor which supports this hypothesis is that in RbCP(Cl) the Pt–Pt distances are also of unequal length (2.924 (8) and 2.877 (8) Å) and RbCP(Cl) has lower room temperature conductivity[4] than KCP(Br). The complete explanation for the structure–conductivity relationships in those POTCP complexes is obviously much more complicated because although a Rb^+ ion has nearly the same cation radius as NH_4^+ and RbCP(Cl) and $NH_4CP(Cl)$ are isostructural, the low-temperature electrical conductivity [$NH_4CP(Cl)$ << RbCP(Cl)] is vastly different.

Acknowledgment. Both A.E.U. and J.M.W. are indebted to N.A.T.O. for a joint research grant (N.A.T.O. Research Grant No. 1276) which made this collaborative work possible. We thank Johnson Matthey and Co., Ltd., for the loan of platinum salts and the Science Research Council for a grant (to D.J.W.).

Registry No. $(NH_4)_2[Pt(CN)_4]\cdot 3H_2O$, 62227-82-1.

Supplementary Material Available: A listing of neutron and x-ray structure factor amplitudes for $NH_4CP(Cl)$ (5 pages). Ordering information is given on any current masthead page.

References and Notes

(1) Work performed under the auspices of the Division of Basic Energy Sciences of the U.S. Department of Energy.
(2) (a) Argonne National Laboratory. (b) University College of North Wales.
(3) For reviews of partially oxidized tetracyanoplatinate compounds see G. D. Stucky, A. J. Schultz, and J. M. Williams, *Annu. Rev. Mater. Sci.*, 7, 301 (1977); J. M. Williams, *Ferroelectrics*, **16**, 135 (1977).

(4) A. E. Underhill, D. M. Watkins, and D. J. Wood, *J. Chem. Soc., Chem. Commun.*, **805** (1976).
(5) A. E. Underhill, D. M. Watkins and D. J. Wood, *J. Chem. Soc., Chem. Commun.*, **392** (1977).
(6) J. M. Williams, P. L. Johnson, A. J. Schultz, and C. C. Coffey, *Inorg. Chem.*, preceding paper in this issue.
(7) J. M. Williams, J. L. Petersen, H. M. Gerdes, and S. W. Peterson, *Phys. Rev. Lett.*, **33**, 1079 (1974); J. M. Williams, F. K. Ross, M. Iwata, J. L. Petersen, S. W. Peterson, S. C. Lin, and K. D. Keefer, *Solid State Commun.*, **17**, 45 (1975); J. M. Williams, M. Iwata, F. K. Ross, J. L. Petersen, and S. W. Peterson, *Mater. Res. Bull.*, **10**, 411 (1975).
(8) J. M. Williams, M. Iwata, S. W. Peterson, K. A. Leslie, and H. J. Guggenheim, *Phys. Rev. Lett.*, **34**, 1653 (1975).
(9) P. Day and J. Hines, *Oper. Syst. Rev.*, **7**, 28 (1973).
(10) S. W. Peterson and H. A. Levy, *Acta Crystallogr.*, **10**, 70 (1957).
(11) The computer programs which were used in performing the necessary calculations with their accession names in the World List of Crystallographic Computer Programs (3rd ed) are as follows: data reduction and absorption corrections, DATALIB; data averaging and sort, DATASORT; Fourier summation, FORDAP; least-squares refinement, ORXFLS3; error analysis of distances and angles, ORFFE3; structural drawings, ORTEPII. For the intensity statistics MULTAN was used: J. P. Declercq, G. Germain, P. Main, and M. M. Woolfson, *Acta Crystallogr., Sect. A*, **29**, 231 (1973).
(12) G. E. Bacon, *Acta Crystallogr., Sect. A*, **8**, 357 (1972).
(13) "International Tables for X-Ray Crystallography", Vol. IV, Kynoch Press, Birmingham, England, 1974, pp 72–98 and (for anomalous dispersion corrections) pp 149–150.
(14) C. Peters and C. F. Eagen, *Phys. Rev. Lett.*, **34**, 1132 (1975); *Inorg. Chem.*, **15**, 782 (1976); H. J. Deiseroth and H. Schulz, *Phys. Rev. Lett.*, **33**, 963 (1974); *Mater. Res. Bull.*, **10**, 225 (1975); G. Heger, B. Renker, H. J. Deiseroth, H. Schulz, and G. Scheiber, *ibid.*, **10**, 217 (1975).
(15) The chemical analyses of $NH_4CP(Cl)$ have yielded slightly conflicting results in terms of the exact Cl^- content. While iodine–thiosulfate titration yielded a Pt oxidation state of 2.28 (1), which because of charge compensation would require $Cl_{0.28}$, the Cl^- chemical analyses[16] consistently yielded $Cl_{0.42\pm0.02}$ if crystals were grown from aqueous NH_4Cl solutions (>3 M). Since the Cl^- occupancy factors determined from the neutron diffraction study are rather imprecise at Cl = 0.4 ± 0.2, it was decided that the best value was $Cl_{0.30}$ which has been determined for the *isostructural* compounds KCP(Br),[7] KCP(Cl),[8] and RbCP(Cl).[6] Because the solutions from which the crystals were prepared are acidic, it is possible that extra halide has been incorporated as $H_3O^+Cl^-$. However, the small amounts of $H_3O^+Cl^-$ required to account for the analytical figure for Cl^- would not be detected in this study.
(16) Franz Pascher, Mikroanalytisches Laboratorium, Bonn, West Germany, and F. B. Strauss, Microanalytical Laboratory, Oxford, England.

Contribution from the Departments of Chemistry,
Barnard College and Columbia University, New York, New York 10027

Transition Metal Hydroborate Complexes. 10.[1] Crystal and Molecular Structure of Tris(tetrahydroborato)tris(tetrahydrofuran)yttrium(III)

BERNICE G. SEGAL*[2a] and STEPHEN J. LIPPARD*[2b]

Received September 8, 1977

The molecular structure of $Y(BH_4)_3(THF)_3$ has been determined by a single-crystal x-ray diffraction study. The complex crystallizes in the space group *Pbcn* of the orthorhombic system, with four molecules per unit cell. Lattice parameters are a = 9.314 (6), b = 14.597 (8), and c = 14.540 (9) Å. The gadolinium analogue $Gd(BH_4)_3(THF)_3$ forms isomorphous crystals. The structure was solved and refined on F to a final value for the discrepancy index R_1 of 0.053, using 804 unique observed reflections collected by diffractometer. The molecular symmetry is crystallographically required to be C_2. The three boron atoms and three oxygen atoms of the THF rings are at the corners of a distorted octahedron centered about the yttrium atom. One of the three tetrahydroborate groups is bidentate and the other two are tridentate. The yttrium atom therefore has a formal coordination number of 11. In the tridentate $Y-BH_4$ attachment, the tetrahydroborate ligand is slightly tilted from local C_{3v} symmetry, resulting in inequivalent Y–H bond lengths. The Y–B distance of 2.68 (2) Å for the bidentate tetrahydroborate ligand is significantly longer than the value of 2.58 (1) Å found for the two tridentate groups. Metal–hydrogen distances are compared with metal–boron distances in 17 tetrahydroborate complexes for which structural data are available. Good agreement is obtained between observed metal–hydrogen distances and values calculated assuming the BH_4^- anion to be a regular tetrahedron bonded to the metal ion with the appropriate bidentate or tridentate coordination.

Introduction

The tetrahydroborate anion, BH_4^-, forms a large variety of covalent complexes with transition metal, lanthanide, and actinide ions. A recent review article[3] summarizes the many reasons for interest in these compounds, which often have properties typical of organic, molecular crystals: low melting points, high vapor pressure, and solubility in nonpolar solvents. The optical, vibrational, and magnetic properties of metal tetrahydroborate complexes have been extensively investigated, and a complete knowledge of their crystal and molecular structures is often necessary to interpret the data. Coordination of the tetrahydroborate anion to the metal ion occurs through bridging hydrogen atoms and can be mono-, bi-, or tridentate (structures I, II, and III). A number of structural

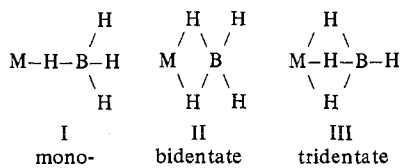

I monodentate II bidentate III tridentate

investigations of tetrahydroborate complexes have appeared recently,[4–6] and the first example of monodentate coordination of the BH_4^- group has just been reported.[7,8]

Most of the tetrahydroborate complexes that have been structurally characterized contain main-group, transition metal, or actinide ions. Recently, several tetrahydroborate complexes with lanthanide or pseudolanthanide ions have been prepared,[9,10] and the optical spectra of mixed crystals of $Er(BH_4)_3(THF)_3/Y(BH_4)_3(THF)_3$, $Er(BH_4)_3(THF)_3/Gd(BH_4)_3(THF)_3$, and $Er(BH_4)_3(THF)_3/La(BH_4)_3(THF)_3$ have been investigated,[10] where THF represents tetrahydrofuran. Knowledge of the crystal structures of $Y(BH_4)_3(THF)_3$, $Gd(BH_4)_3(THF)_3$, and $La(BH_4)_3(THF)_3$ will aid in the interpretation of the optical spectra. To provide this information and to probe further the factors that govern bidentate vs. tridentate coordination of the small, anionic BH_4^- ligand to metals, an x-ray diffraction study of one of these lanthanide or pseudolanthanide tetrahydroborate complexes was undertaken. The yttrium complex was chosen because its significantly smaller electron density compared with that of the lanthanides facilitates location of hydrogen atom positions.

Nuclear magnetic resonance studies have shown that for both bidentate and tridentate coordination, in almost all known tetrahydroborate complexes, there is a dynamic intramolecular rearrangement process that rapidly interchanges bridging and terminal hydrogens. One mechanism proposed[11,12] for this

0020-1669/78/1317-0844$01.00/0